AD

TECHNICAL REPORT ARCCB-TR-02017

UPDATED EROSION MODELING PREDICTIONS FOR THE M829E3 ROUND

S. SOPOK
G. PFLEGL
C. RICKARD

DECEMBER 2002

20030210 097

REPORT DOCUMENTATION PAGE

Public reporting burden for this collection of information is estimated to average 1 hour per response, including the time for reviewing instructions, searching existing data sources, gathering and maintaining the data needed, and completing and reviewing the collection of information. Send comments regarding this burden estimate or any other aspect of this collection of information, including suggestions for reducing this burden, to Washington Headquarters Services, Directorate for Information Operations and Reports, 1215 Jefferson Davis Highway, Suite 1204, Arlington, VA 22202-4302, and to the Office of Management and Budget, Paperwork Reduction Project (0704-0188), Washington, DC 20503.

1. AGENCY USE ONLY (Leave Blank)	2. REPORT DATE December 2002	3. REPORT TYPE AND DATES COVERED Final

4. TITLE AND SUBTITLE
UPDATED EROSION MODELING PREDICTIONS FOR THE M829E3 ROUND

5. FUNDING NUMBERS
AMCMS No. 6226.24.H180.0
PRON No. 4AZC2FYK1ABJ

6. AUTHORS
S. Sopok, G. Pflegl, and C. Rickard

7. PERFORMING ORGANIZATION NAME(S) AND ADDRESS(ES)
U.S. Army ARDEC
Benet Laboratories, AMSTA-AR-CCB-O
Watervliet, NY 12189-4000

8. PERFORMING ORGANIZATION REPORT NUMBER
ARCCB-TR-02017

9. SPONSORING / MONITORING AGENCY NAME(S) AND ADDRESS(ES)
U.S. Army ARDEC
Close Combat Armaments Center
Picatinny Arsenal, NJ 07806-5000

10. SPONSORING / MONITORING AGENCY REPORT NUMBER

11. SUPPLEMENTARY NOTES
Presented at the 38th JANNAF Combustion Meeting, Destin, FL, 8-12 April 2002.
Published in proceedings of the meeting.

12a. DISTRIBUTION / AVAILABILITY STATEMENT
Approved for public release; distribution unlimited.

12b. DISTRIBUTION CODE

13. ABSTRACT (Maximum 200 words)

Erosion modeling predictions are given for the current M829E3 round configuration and weighted averages per temperature for the computer correction factor (CCF). Our gun erosion model was developed through a ten-year joint partnership with Software and Engineering Associates, Inc., Carson City, NV. These predictions are based on recent cannon characterization data. These latest predictions include significant changes in propellant configuration and projectile weight that were made to the current M829E3 configuration compared to our initially presented M829E3 modeling predictions two years ago. For the last two years, additional nonablative M829E3 erosion modeling predictions have not been conducted or presented. This was due to a diversion of erosion modeling resources toward ablative M829E3 erosion predictions and erosion predictions related to the selection of six M256 cannons for M829E3-related fatigue testing. For the current M829E3 configuration, these changes in gas pressure, gas temperature, gas velocity, and increased projectile weight collectively contributed to a predicted increase in M256 cannon erosion life compared to our initially presented M829E3 modeling effort. In addition, the current set of M829E3 weighted averages per temperature for CCF from Fort Knox (19% hot 49°C/120°F, 64% basic 21°C/70°F, 16% cold -7°C/20°F, and 1% severe -32°C/-25°F) collectively contributed to a further predicted increase in M256 cannon erosion life compared to the two-year-old set of weighted averages per temperature (33% hot, 33% basic, 0% cold, and 33% severe). For the current predictions, the peak eroded cannon axial position remains at approximately 60 inches from the rear face of the tube ±6 inches; and this position dictates the erosion life of the cannon. Erosion life predictions at this position are given for each of the round-conditioning temperatures and the Fort Knox mixture of round-conditioning temperatures. At this peak eroded position, the respective 49°C/120°F, 21°C/70°F, -7°C/20°F, -32°C/-25°F, and Fort Knox mixture round-conditioning temperature cases have predicted erosion lives of approximately 183, 287, 388, 302, and 269 rounds. The mixture of M829E3 rounds with some types of HEAT and slug rounds significantly moves the peak eroded axial position up-bore to the bore onset region.

14. SUBJECT TERMS
Erosion Modeling, M256 Cannon, M829E3 Round, Erosion Predictions

15. NUMBER OF PAGES
17

16. PRICE CODE

17. SECURITY CLASSIFICATION OF REPORT UNCLASSIFIED	18. SECURITY CLASSIFICATION OF THIS PAGE UNCLASSIFIED	19. SECURITY CLASSIFICATION OF ABSTRACT UNCLASSIFIED	20. LIMITATION OF ABSTRACT UL

AQM03-04-0950

TABLE OF CONTENTS

LIST OF ILLUSTRATIONS

INTRODUCTION

Our initial cannon erosion model was introduced seven years ago and was quite successful at predicting progressive bore erosion (ref 1). Progressive erosion generally occurs for uncoated steel and nitrided steel cannon bores. The following year we modified this initial cannon erosion model into our cannon coating erosion model and presented it in-house. We publicly presented our cannon coating erosion model after it had stood the test of time for a wide spectrum of gun system types (ref 2). The modified model successfully predicts erosion for coated steel bores and the effects of bore-protecting ablatives. For the last six years, we have presented many cannon coating model predictions for a wide array of important Army and Navy gun systems with bore coatings and, if applicable, ablatives.

We presented our initial M256/M829E3 cannon coating erosion modeling predictions for an experimental configuration of the PM-TMAS M829E3 round three years ago (ref 3). This configuration included 19 pounds of RPD-380 propellant, a classified projectile slug weight (version F), and the absence and presence of 1.0 pound of ablative paste on a moving projectile base donut. This RPD-380 propellant was not allowed to fracture at -32°C despite its glass transition at -29°C. In addition, if the ablative paste products were present, they were not allowed to deposit on the cannon bore surface. Significant live firing of this round configuration showed these predictions to be valid.

Two years ago, we presented more M256/M829E3 cannon coating erosion modeling predictions for another experimental configuration of the PM-TMAS M829E3 round (ref 2). This configuration included 18 pounds of RPD-380 propellant, a 0.3-pound lighter weight classified projectile slug (version F) than the initial modeled projectile, and no ablative paste. This RPD-380 propellant was allowed to fracture at -32°C due to its glass transition at -29°C. Again, significant live firing of this round configuration showed these predictions to be valid.

Also two years ago, we presented additional M256/M829E3 cannon coating erosion modeling predictions for yet another experimental configuration of the PM-TMAS M829E3 round (ref 4). This configuration included 18 pounds of RPD-380 propellant, 0.3-pound lighter weight classified projectile slug (version F) than the initial modeled projectile, and 0.5-pound of ablative paste on the combustible case shoulder. Again, this RPD-380 propellant was allowed to fracture at -32°C due to its glass transition at -29°C. In addition, ablative paste products were allowed to deposit on the cannon bore surface. Limited live firing of this round configuration showed evidence that these predictions are valid.

For the last two years, additional nonablative M829E3 erosion modeling predictions have not been conducted or presented. This was due to a diversion of erosion modeling resources toward ablative M829E3 erosion predictions and erosion predictions related to the selection of six M256 cannons for M829E3-related fatigue testing.

For this current effort, erosion modeling predictions are given for the current M829E3 round configuration and weighted averages per temperature for the computer correction factor (CCF). They are based on recent cannon characterization data presented two years ago. These

latest predictions include significant changes in propellant configuration and increased projectile weight that were made to the current M829E3 configuration compared to our initially presented M829E3 modeling predictions. These latest predictions also include significant changes in the weighted averages per temperature for CCF that were applied to the current M829E3 round compared to our initially presented M829E3 modeling predictions.

COMPUTATIONAL AND EXPERIMENTAL METHODS

Our cannon coating erosion model is used to predict wall temperature profiles and thermal-chemical-mechanical erosion profiles in bore-coated cannons as a function of position, time, and round history. This overall model is comprised of a number of interactively linked submodels (refs 1,2,4-8). These submodels include:

- CCET thermochemistry cannon model (refs 1,2,4,5)
- XNOVAKTC interior ballistics model (refs 1,2,4,6)
- MABL boundary layer cannon model (refs 1,2,4,7)
- MACE thermal and erosion cannon model (refs 1,2,4,8)

These erosion predictions are guided and calibrated by substantial gun system firing data and fired cannon specimen analyses. The M829E3 modeling effort uses 18 pounds of RPD-380 propellant. This current M829E3 round configuration introduced significant changes in propellant configuration and increased projectile weight compared to our initially presented M829E3 modeling predictions two years ago. In addition, there are significant changes in the weighted averages per temperature for CCF applied to the current M829E3 round compared to our initially presented M829E3 modeling predictions. This RPD-380 propellant was allowed to fracture at -32°C temperature condition due to its glass transition at -29°C.

Pressure gauge, radar, thermocouple, and kinetic rate data are used to calibrate these models. These models receive important inputs for nondestructive and laboratory microscopic material and chemical analyses of fired cannon specimens. The analyses focus on substrate exposure, coating loss, cracks, pits, interfaces, voids, and surfaces including their crack/pit frequency, crack/pit width, coating platelet width, wall layers, residues, reactions, diffused species, and phase changes all as a function of position, time, and round history.

RESULTS AND DISCUSSION

Our overall erosion modeling analysis for the current configuration of the PM-TMAS experimental M829E3 round fired from the M256 cannon begins with the CCET thermochemistry cannon model. It uses chemical and material inputs to calculate gas/gas thermochemistry data for the interior ballistics, boundary layer, and thermal and erosion codes. Its RPD-380 propellant consists of approximately 59% nitrocellulose, 25% nitroglycerine, 15% diethylene glycol dinitrate, 1% other minor species, and 50 grams of igniter. Measured thermochemical data are used to calibrate the calculation for gas/gas products.

The XNOVAKTC interior ballistics model uses thermochemistry code output and gun system defining inputs to calculate the time-dependent core flow data for the boundary layer code. This gun system includes the 17.3-foot 120-mm M256 cannon, its experimental 18-pound RPD-380 propellant, and classified projectile details. Measured pressure gauge and muzzle velocity data are used to calibrate this time-dependent core flow calculation.

Figures 1 and 2 give XNOVAKTC interior ballistic model results for the current configuration of the experimental M829E3 round. These figures respectively give maximum values of gas pressure (P_g) and gas temperature (T_g) as a function of selected axial positions at selected round-conditioning temperatures. Maximum values were used instead of time-dependent data to compare the various round-conditioning temperature cases. Both P_g and T_g decrease with increasing axial position. Gas velocity is omitted due to its classified nature. Selected axial positions included 0.6, 1.6, 2.2, 3.3, and 5.1 meters from the rear face of the tube (RFT), while the selected round-conditioning included the hot 49°C/120°F, basic 21°C/70°F, cold -7°C/20°F, and severe -25°F/-32°C temperatures. These five selected axial positions and four selected round-conditioning temperatures are used exclusively throughout the rest this report. In addition, the current set of M829E3 weighted averages per temperature for CCF from Fort Knox include 19% hot 49°C/120°F, 64% basic 21°C/70°F, 16% cold -7°C/20°F, and 1% severe -25°F/-32°C.

In these first two figures, the significance of the 0.6-meter position is that it is slightly past the origin of the bore, and it is the mean peak eroded position when both M829E3 and some types of HEAT and slug rounds are mixed. The significance of the 1.6-meter position is that it is the mean peak eroded position when M829E3 rounds are fired without a mixture of these HEAT or slug rounds. The significance of the 2.2-meter position is that it is the mean peak eroded position when M829A2 rounds are fired in the M256 cannon without a mixture of these HEAT or slug rounds. The significance of the 3.3-meter position is that it is near the bore evacuator holes. The significance of the 5.1-meter position is that it is near the muzzle. Statistical distributions exist around these predictions for the various eroded positions. This effort concentrates on the current configuration of the experimental M829E3 round fired without a mixture of these HEAT or slug rounds.

The MABL boundary layer cannon model uses thermochemistry and interior ballistics model outputs to calculate boundary layer characteristics for the thermal and erosion model. Figures 3 and 4 give the MABL boundary layer model results for the current configuration of the experimental M829E3 round. These figures respectively give maximum values of recovery enthalpy (H_r) and cold wall heat flux (Q_{cw}) as a function of selected axial positions at selected round-conditioning temperatures. Maximum values were again used instead of time-dependent data to compare the four round-conditioning temperatures. In these figures, both H_r and Q_{cw} increase with increasing axial position to a 1.6-meter from RFT peak and decrease thereafter to the muzzle. The 0.6-meter from RFT peak heat transfer position calculated by the interior ballistics analysis is shifted to a 1.6-meter from RFT peak position due to the added boundary layer analysis inclusion of the 1600°K combustible case gas cooling effects and turbulent gas mixing and heating effects.

3

The CCET thermochemistry cannon model uses initial chemical and materials input to calculate gas/wall thermochemistry data for the thermal and erosion code. Measured thermochemical data are used to calibrate the calculation for gas/wall products and gas/wall reaction rates. Figure 5 gives the CCET thermochemical model results for the current configuration of the experimental M829E3 round. Simplified mean values are given for the reacting gas/wall enthalpy (H_{gw}) and thermochemical ablation potential (B_a) as a function of wall temperatures (T_{wall}) for the high contraction (HC) chromium plate/gun steel substrate wall materials.

The MACE thermal and erosion cannon model uses thermochemistry model output, boundary layer model output, material properties input, and firing history and scenario input to calculate wall temperature profiles and thermal-chemical-mechanical wall erosion profiles. These predicted results are given as a function of axial position, radial position, time, and firing history and scenario.

The following data types are used to calibrate the wall thermal and erosion calculation:

- Experimentally measured gas/wall kinetic rate function input data
- Measured thermocouple input data
- Measured destructive/nondestructive microscopic coating and steel loss (void) input data (cracks, pits, interfaces, surfaces)
- Measured destructive reaction/diffusion/phase change degradation layer input data (cracks, pits, interfaces, surfaces)

Experimentally measured gas/wall kinetic rate function data are used to calibrate the thermochemical calculation and transform this chemical equilibrium calculation into a partial chemical kinetic calculation. Chemical analysis of crack and pit wall layers, interface wall layers, bore surface layers, subsurface void residues, and surface residues further guide this gas/wall kinetics calibration. Thermocouple data are used to calibrate the wall thermal profile calculation.

Based on the latest cannon characterization data for the experimental M829E3 round, Figure 6 gives typical gun steel substrate exposure for the M256 cannon. These data are from a small sampling of HC chromium plated M256 cannons that have typical cracking, pitting, and chromium plate loss. This small sampling of cannons was condemned on erosion and had numerous condemning scoring holes centered at the 1.6-meter from RFT position. The substrate exposure is a function of the selected axial positions at 1% (nondestructively measured at post-proofing), 50% (exponentially estimated), 80% (exponentially estimated), and 100% (nondestructively and destructively measured at erosion condemnation) of equivalent ambient-conditioned M829E3 erosion life based on previous work (ref 2).

The nondestructive substrate exposure measurements are taken by a magnifying borescope with a calibrated scale, while the corresponding destructive measurements are taken by metallographic and scanning electron microscopic techniques. These nondestructive measurements are based on the verified assumption that substrate exposure is approximately

4

equal at the surface and interface. Bore position-dependent and equivalent erosion life-dependent substrate exposure measurements of specimens from fired cannons include axial and circumferential crack/pit frequency, axial and circumferential crack/pit width, and axial and circumferential platelet width. The measured substrate exposure pattern correlates with the boundary layer heat transfer pattern where both increase with increasing axial position to a 1.6-meter from RFT peak and decrease thereafter to the muzzle.

Figures 7 and 8 show micrographic examples of destructive substrate exposure measurements. These measurements were taken by metallographic and scanning electron microscopic techniques. For the experimental M829E3 round peak-eroded position of 1.6 meters from RFT, these micrographs respectively illustrate typical enabling and accelerating erosion mechanism steps. Figure 7 shows a very fine HC chromium plate crack that provides a narrow combustion gas path to the gun steel producing limited interfacial gun steel degradation. Figure 8 shows a progressively widened/extended HC chromium plate crack due to chromium shrinkage that provides a wide combustion gas path to the gun steel producing substantial interfacial gun steel degradation, which leads to eventual spalling of the associated chromium platelet. Using these techniques, coupled with their associated chemical analysis techniques, these and similar micrographs illustrate phase change degradation (diffusion-induced carburized white layer and heat-affected zone on/into exposed gun steel, chromium recrystallization) and chemical reaction degradation (oxygen and sulfur oxidation of exposed gun steel forming semi-metallic layers) of the gun steel substrate under the 130-μm thick chromium plate and particularly at crack and interfacial walls/wall layers.

For the current configuration of the experimental M829E3 round, Figures 9 through 11 show the respective maximum wall temperature (T_{wall}) results for the HC chromium surface, gun steel interface, and gun steel surface minus 0.13-mm as a function of the selected axial positions at the selected round-conditioning temperatures. For these figures, maximum values were also used instead of time-dependent data to compare round-conditioning temperatures. The calculated maximum wall temperature patterns correlate with the boundary layer heat transfer patterns, where both increase with increasing axial position to a 1.6-meter from RFT peak and decrease thereafter to the muzzle. The initial wall degradation temperature for the HC chromium surface is not reached, thus explaining its inertness. Numerous wall degradation temperatures for both the unexposed nonreacting gun steel interface and the fully exposed reacting gun steel surface (bore minus 0.13-mm) are reached, thus explaining their reactivity.

Data from Figures 6 and 9 through 11 are used to calibrate and predict resultant substrate interface temperatures for given crack/pit widths using a cubic function (ref 2). These data include the fully convective/exposed surface heating case from Figures 9 and 11, the fully conductive/unexposed substrate interface heating case from Figure 10, and the substrate exposure data from Figure 6. Using this cubic function, Figure 12 presents the substrate interface temperatures for given crack/pit widths for the current configuration of the experimental M829E3 round. These data consist of the maximum exposed interface temperature as a function of HC chromium crack/pit width at selected axial positions and 49°C round conditioning.

5

These resultant substrate interface temperatures for given crack/pit widths correlate and have been successfully applied to numerous advanced medium and large caliber gun systems based on measured firing-related data from their most extreme rounds. The measurements include phase change degradation data (diffusion-induced carburized white layer and heat-affected zone on/into exposed gun steel, chromium recrystallization) and chemical reaction degradation data (oxygen and sulfur oxidation of exposed gun steel forming semi-metallic layers). The existence and depth of these measured degradations into the exposed gun steel substrate depend on and correlate with the magnitude of the related positional-dependent wall temperature profiles. These measurements were particularly focused on the exposed gun steel substrate at the crack/pit/interface walls and wall layers.

Surface ablation rates are calculated directly by the MACE model. The MACE model also uses the resultant substrate interface temperatures in cracks/pits to calculate the substrate interface ablation rates as a function of position, time, and rounds. This is done for the life of each crack and pit. The exposed steel interface degradation (transformation, interstitial occupation, and reactions) under a chromium platelet is consumed by the associated ablation rate above the ablation threshold. When any type of degradation of the exposed gun steel interface thickness under this coating platelet merges from all adjacent cracks/pits, then the coating platelet spalls and gas wash onset begins.

The HC chromium plate has a passivating oxidation at about 2000°K and a melting point at about 2130°K, both of which explain its inertness. Steel substrate degradation of interfaces, cracks, pits, and surfaces is computed by the area under a temperature-time curve above a degradation threshold such as:

- The 1000°K transformation onset of steel
- The 1050°K accelerated expansive flaking scale-type oxidation onset of iron by oxygen
- The 1050°K accelerated diffusion of carbon into steel to Fe3C
- The 1270°K accelerated oxidation onset of iron by sulfur
- The 1420°K melting point onset of iron carbide white layer eutectic
- The 1470°K melting point onset of the iron-sulfur compound
- The 1640°K melting point onset of the iron-oxygen compound
- The 1720 K melting point onset of gun steel

Calibrated diffusion controlled transformation codes are used to evaluate multi-component gun steel system transformations.

Using nondestructive and laboratory microscopic materials/chemical analyses of fired cannon specimens, it is important to measure the achievement of and level above these reaction thresholds as a function of position, time, and round history. This bore coating erosion model requires measurable gas/wall bore coating and steel substrate reactivity data as a function of pressure, temperature, and velocity. These data are from the literature and in-house measurements for each gun system material/configuration using specialized gas/wall kinetic rate testers.

Figures 13 and 14 show the cumulative erosion predictions for the current configuration of the experimental M829E3 round. These predictions include the respective values of cumulative rounds to 0.13-mm erosion (coating micropitting onset) and 5-mm erosion (bore erosion condemnation) as a function of the selected axial positions at selected round-conditioning temperatures. The data in these two figures inversely correlate with the above boundary layer heat transfer and substrate exposure patterns. These erosion patterns decreased to a 1.6-meter from RFT minimum and increased thereafter. In Figure 13, the chromium plate loss at the muzzle is due to purely mechanical effects. Figure 15 gives a summary of Figures 13 and 14 at the erosion condemnation governing the 1.6-meter from RFT peak eroded position. This last figure gives cumulative erosion versus cumulative equivalent M829E3 rounds at 1.6 meters from the RFT.

For the current M829E3 configuration, changes in gas pressure, gas temperature, gas velocity, and increased projectile weight collectively contributed to a predicted increase in M256 cannon erosion life. This increase in erosion life has been compared to our initially presented M829E3 modeling effort two years ago, which had a different M829E3 configuration. In addition, the current set of M829E3 weighted averages per temperature for CCF from Fort Knox (19% hot 49°C/120°F, 64% basic 21°C/70°F, 16% cold -7°C/20°F, and 1% severe -25°F/-32°C) collectively contributed to a further predicted increase in M256 cannon erosion life compared to the two-year-old set of weighted averages per temperature (33% hot, 33% basic, 0% cold, and 33% severe). For the current predictions, the peak eroded cannon axial position remains at approximately 60 inches from the RFT ±6 inches, and this position dictates the erosion life of the cannon. Erosion life predictions at this position are given for each of the round-conditioning temperatures and the Fort Knox mixture of round-conditioning temperatures based on the 5-mm erosion condemnation criteria. At this peak eroded position, the respective 49°C/120°F, 21°C/70°F, -7°C/20°F, -32°C/-25°F, and Fort Knox mixture round-conditioning temperature cases have predicted erosion lives of approximately 183, 287, 388, 302, and 269 rounds.

Predictions for the current configuration of the experimental M829E3 round apply to cannons with a mixture of M829E3 rounds and other kinetic energy-type rounds. When some types of HEAT and slug rounds are added to this mixture, their documented fin gouging of the bore produces additional/higher frequency HC chromium cracking/pitting. This fin gouging occurs in the latter forcing cone and the first 0.3-meter of bore travel past the forcing cone, and is not present when these HEAT and slug rounds are absent. For the M829E3 round, the presence of HEAT and slug round gouging produces peak erosion at the 0.6-meter from the RFT position instead of the normal 1.6-meter from RFT peak eroded position when these HEAT and slug rounds are absent.

REFERENCES

1. Dunn, S., Sopok, S., Coats, D., O'Hara, P., Nickerson, G., and Pflegl, G., "Unified Computer Model for Predicting Thermochemical Erosion in Gun Barrels," *Proceedings of 31st AIAA Joint Propulsion Conference*, San Diego, CA, July 1995; Also *AIAA Journal of Propulsion and Power*, Volume 15, Number 4, pp. 601-612.

2. Sopok, S., "Cannon Coating Erosion Model with Updated M829E3 Example," *Proceedings of 36th AIAA Joint Propulsion Conference*, Huntsville, AL, July 2000.

3. Sopok, S., Loomis, R., Pflegl, G., and Rickard, C., "Preliminary Erosion Analysis for the Experimental M829E3 Kinetic Energy Round," *Proceedings of the 36th JANNAF Combustion Meeting*, NASA Kennedy Space Center, FL, October 1999.

4. Sopok, S., and Fleszar, M., "Ablative Erosion Model for the M256/M829E3 Gun System," *Proceedings of the 37th JANNAF Combustion Meeting*, Monterey, CA, November 2000.

5. Coats, D., Dunn, S., and Sopok, S., "A New Chemical Equilibrium Code with Compressibility Effects," *Proceedings of the 33rd JANNAF Combustion Meeting*, Monterey, CA, October 1996.

6. Gough, P., "The XNOVAKTC Code," Paul Gough Associates, Portsmouth, NH, U.S. Army BRL-CR-627, February 1990. Developed and distributed by the Army Research Laboratory, APG, MD.

7. Levine, J., "Transpiration and Film Cooling Boundary Layer Computer Program (MABL) - Numerical Solution of the Turbulent Boundary Layer Equations with Equilibrium Chemistry," NASA Marshall N72-19312, June 1971; Also Dunn, S., "MABL Gun Model," Software and Engineering Associates, Inc., Carson City, NV, February 1992.

8. Dunn, S., "Materials Ablation Conduction Erosion Program (MACE)," Software and Engineering Associates, Inc., Carson City, NV, June 1989; Also Dunn, S., "Updated MACE Gun Model," Software and Engineering Associates, Inc., Carson City, NV, February 1992.
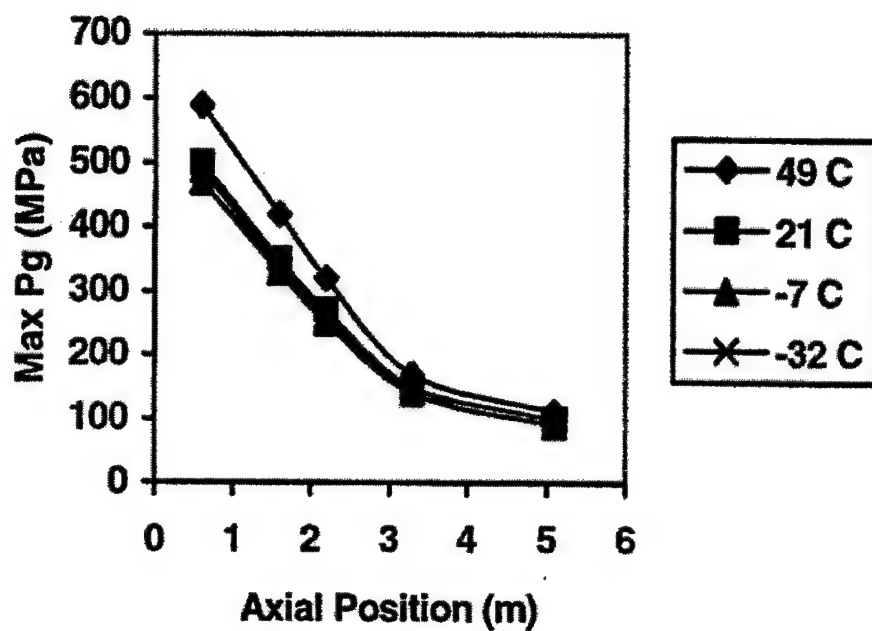
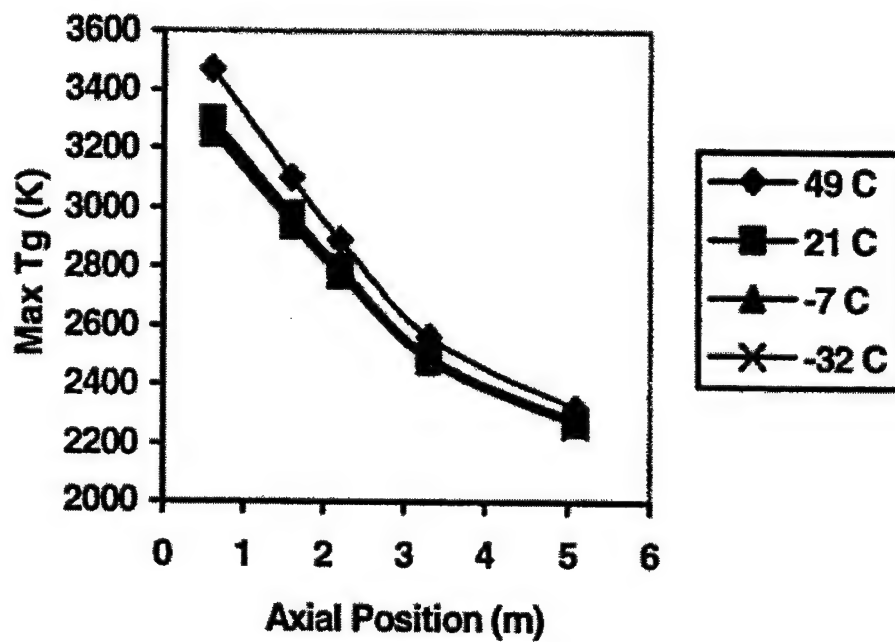Figure 1. M829E3 NOVA gas pressure.
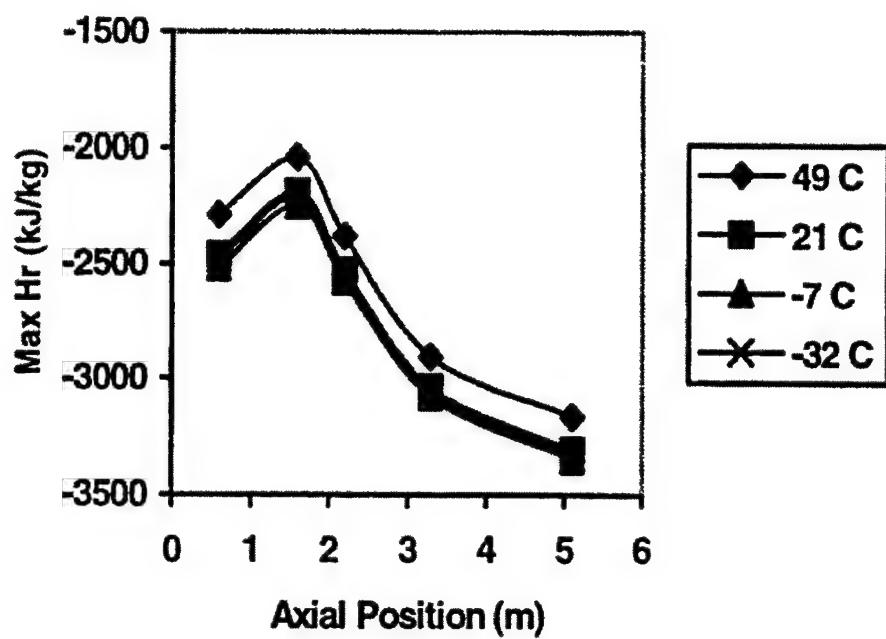

Figure 2. M829E3 NOVA gas temperature.

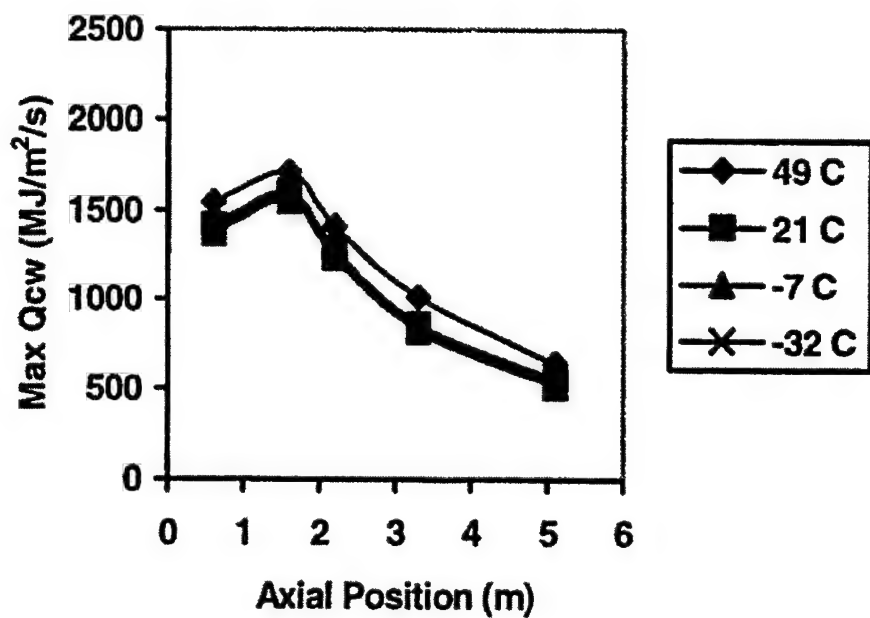Figure 3. M829E3 MABL recovery enthalpy.
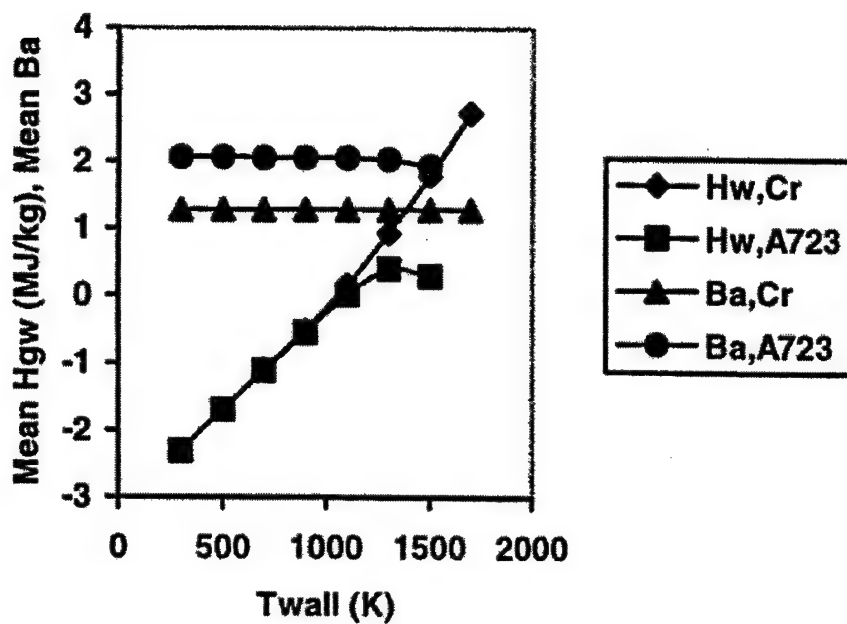

Figure 4. M829E3 MABL cold wall heat flux.

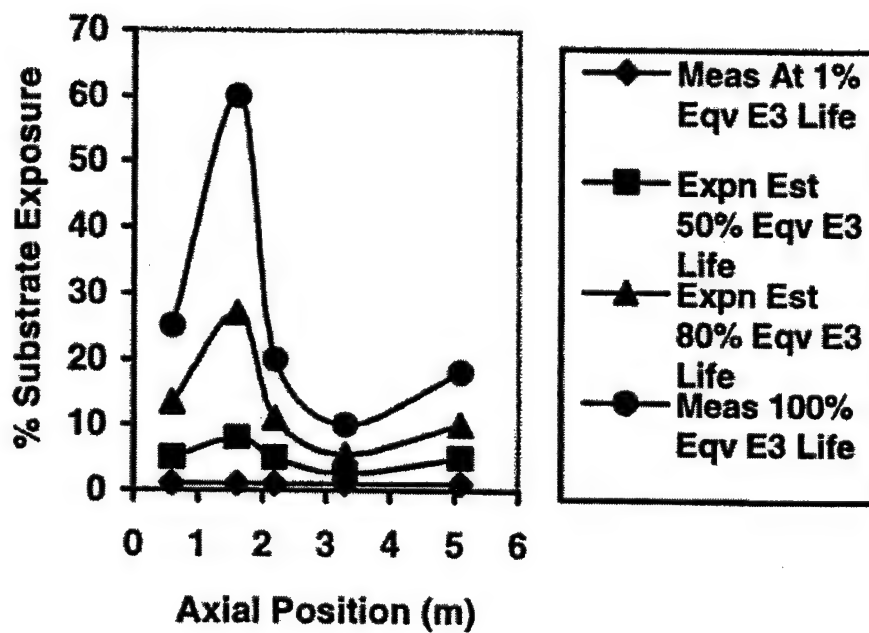Figure 5. M829E3 CCET gas/wall thermochemistry.
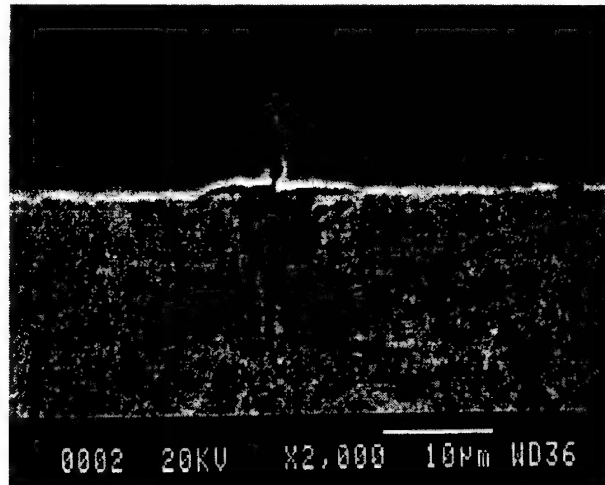

Figure 6. M829E3 M256 substrate exposure.
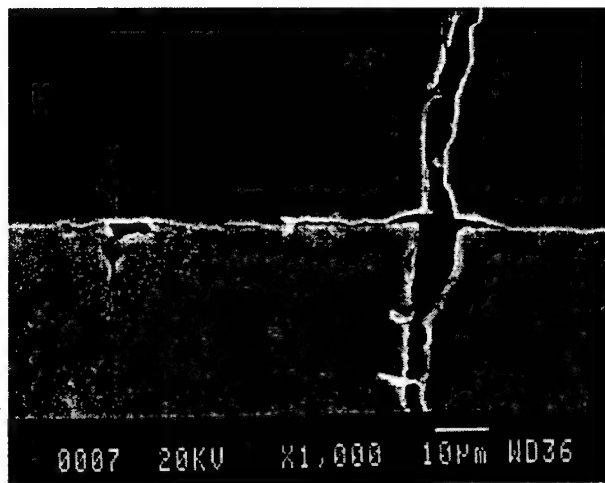
Figure 7. M829E3 enabling erosion example.
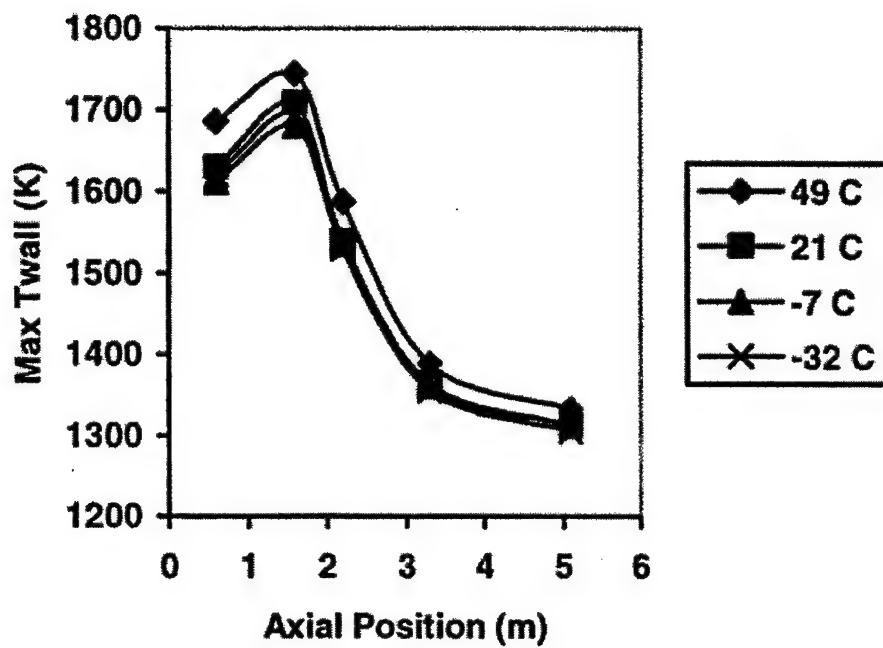

Figure 8. M829E3 accelerating erosion example.
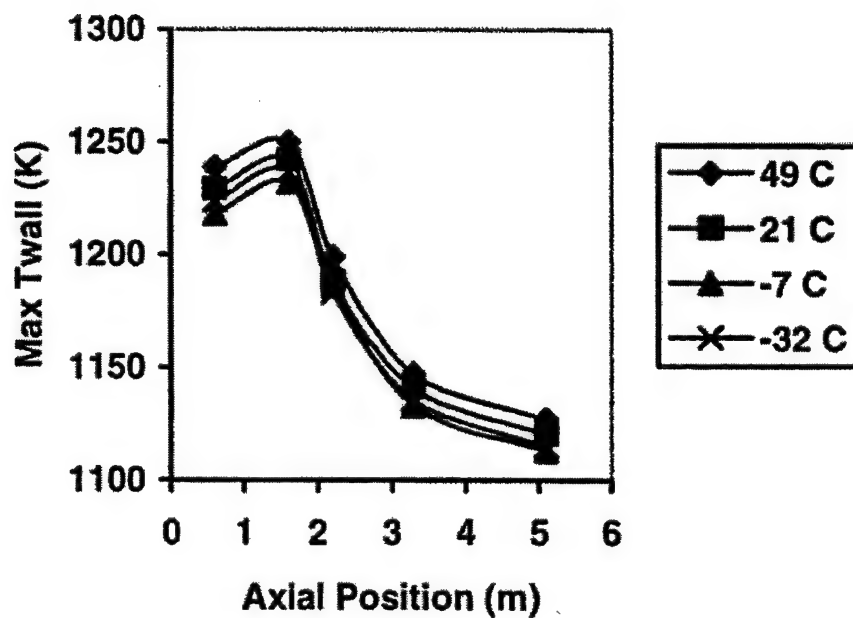
Figure 9. M829E3 MACE HC chromium surface temperature.
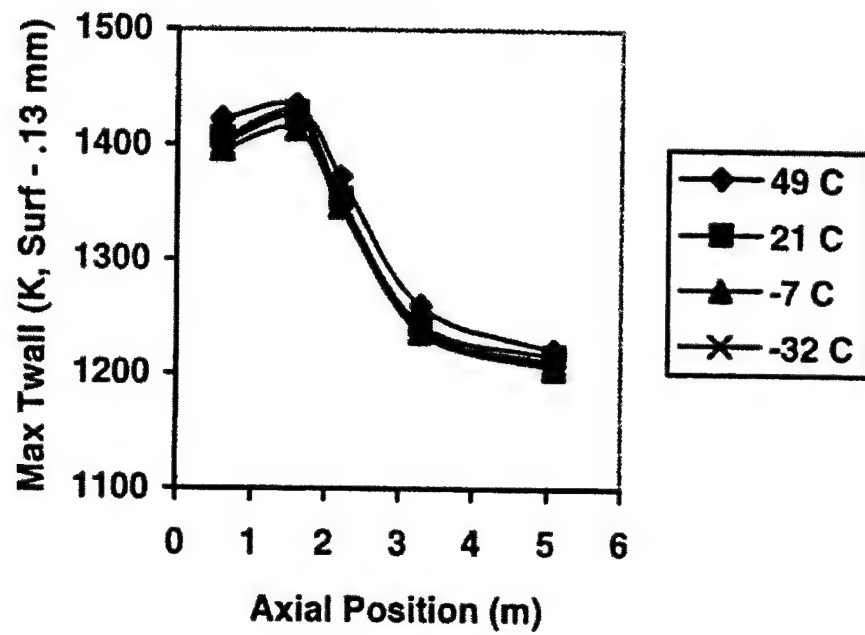

Figure 10. M829E3 MACE A723 interface temperature.

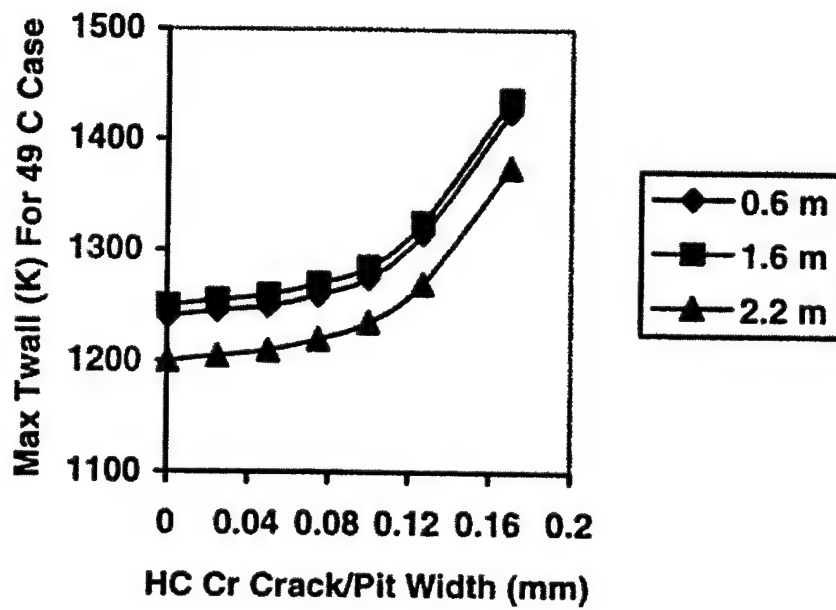Figure 11. M829E3 MACE A723 surface temperature.
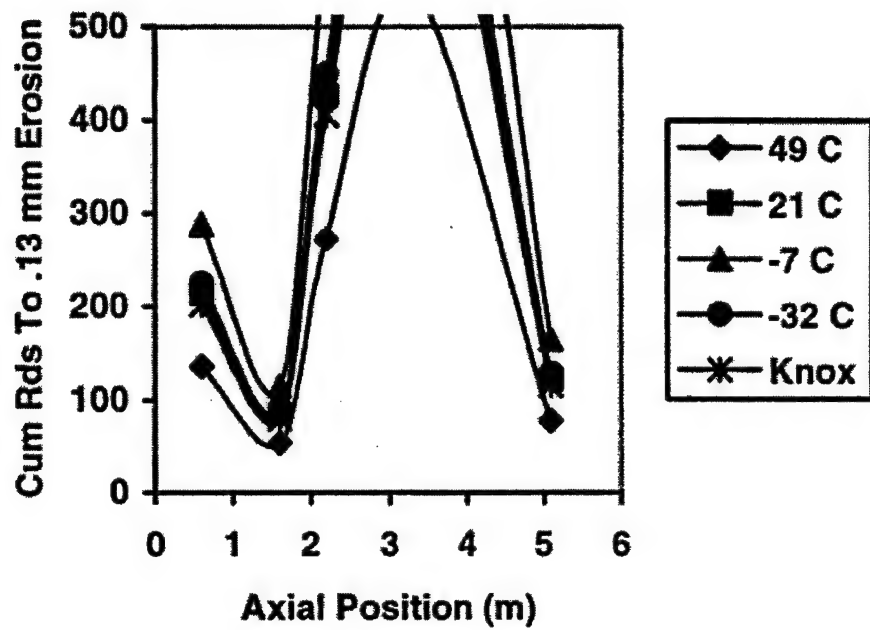
Figure 12. M829E3 exposed interface temperature.
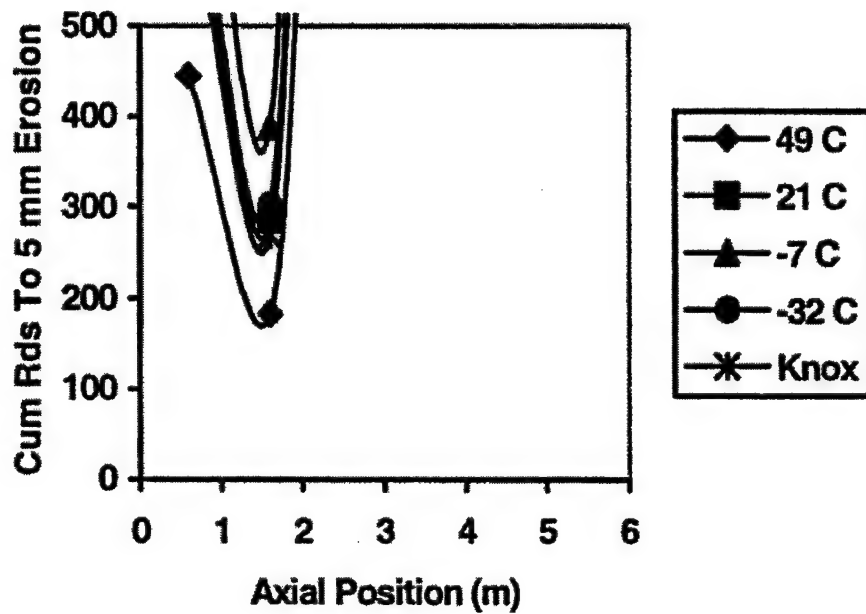
Figure 13. M829E3 erosion micropitting onset.
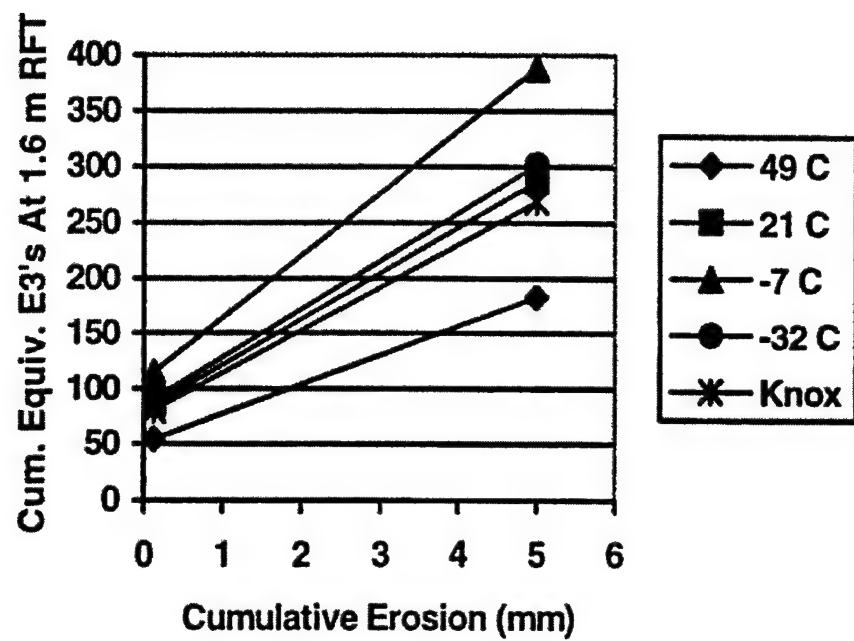

Figure 14. M829E3 erosion condemnation.

Figure 15. M829E3 erosion summary.

TECHNICAL REPORT INTERNAL DISTRIBUTION LIST

	NO. OF COPIES
TECHNICAL LIBRARY ATTN: AMSTA-AR-CCB-O	1
TECHNICAL PUBLICATIONS & EDITING SECTION ATTN: AMSTA-AR-CCB-O	3
PRODUCTION PLANNING & CONTROL DIVISION ATTN: SOSWV-ODP-Q, BLDG. 35	1

NOTE: PLEASE NOTIFY DIRECTOR, BENÉT LABORATORIES, ATTN: AMSTA-AR-CCB-O OF ADDRESS CHANGES.

TECHNICAL REPORT EXTERNAL DISTRIBUTION LIST

	NO. OF COPIES		NO. OF COPIES
DEFENSE TECHNICAL INFO CENTER ATTN: DTIC-OCA (ACQUISITIONS) 8725 JOHN J. KINGMAN ROAD STE 0944 FT. BELVOIR, VA 22060-6218	2	COMMANDER U.S. ARMY RESEARCH OFFICE ATTN: TECHNICAL LIBRARIAN P.O. BOX 12211 4300 S. MIAMI BOULEVARD RESEARCH TRIANGLE PARK, NC 27709-2211	1
COMMANDER U.S. ARMY ARDEC ATTN: AMSTA-AR-WEE, BLDG. 3022 AMSTA-AR-AET-O, BLDG. 183 AMSTA-AR-FSA, BLDG. 61 AMSTA-AR-FSX AMSTA-AR-FSA-M, BLDG. 61 SO AMSTA-AR-WEL-TL, BLDG. 59 PICATINNY ARSENAL, NJ 07806-5000	1 1 1 1 1 2	COMMANDER ROCK ISLAND ARSENAL ATTN: SIORI-SEM-L ROCK ISLAND, IL 61299-5001	1
DIRECTOR U.S. ARMY RESEARCH LABORATORY ATTN: AMSRL-DD-T, BLDG. 305 ABERDEEN PROVING GROUND, MD 21005-5066	1	COMMANDER U.S. ARMY TANK-AUTMV R&D COMMAND ATTN: AMSTA-DDL (TECH LIBRARY) WARREN, MI 48397-5000	1
DIRECTOR U.S. ARMY RESEARCH LABORATORY ATTN: AMSRL-WM-MB (DR. B. BURNS) ABERDEEN PROVING GROUND, MD 21005-5066	1	COMMANDER U.S. MILITARY ACADEMY ATTN: DEPT OF CIVIL & MECH ENGR WEST POINT, NY 10966-1792	1
CHIEF COMPOSITES & LIGHTWEIGHT STRUCTURES WEAPONS & MATLS RESEARCH DIRECT U.S. ARMY RESEARCH LABORATORY ATTN: AMSRL-WM-MB (DR. BRUCE FINK) ABERDEEN PROVING GROUND, MD 21005-5066	1	U.S. ARMY AVIATION AND MISSILE COM REDSTONE SCIENTIFIC INFO CENTER ATTN: AMSAM-RD-OB-R (DOCUMENTS) REDSTONE ARSENAL, AL 35898-5000	2
		COMMANDER U.S. ARMY FOREIGN SCI & TECH CENTER ATTN: DRXST-SD 220 7TH STREET, N.E. CHARLOTTESVILLE, VA 22901	1

NOTE: PLEASE NOTIFY COMMANDER, ARMAMENT RESEARCH, DEVELOPMENT, AND ENGINEERING CENTER,
BENÉT LABORATORIES, CCAC, U.S. ARMY TANK-AUTOMOTIVE AND ARMAMENTS COMMAND,
  AMSTA-AR-CCB-O, WATERVLIET, NY 12189-4050 OF ADDRESS CHANGES.

DISCLAIMER

The findings in this report are not to be construed as an official Department of the Army position unless so designated by other authorized documents.

The use of trade name(s) and/or manufacturer(s) does not constitute an official endorsement or approval.

DESTRUCTION NOTICE

For classified documents, follow the procedures in DoD 5200.22-M, Industrial Security Manual, Section II-19, or DoD 5200.1-R, Information Security Program Regulation, Chapter IX.

For unclassified, limited documents, destroy by any method that will prevent disclosure of contents or reconstruction of the document.

For unclassified, unlimited documents, destroy when the report is no longer needed. Do not return it to the originator.